ASSESSING EMBANKMENT DAM SLOPE STABILITY, PORE PRESSURE, RESERVOIR EMPTYING AND EARTHQUAKE-INDUCED STRESSES: A CASE STUDY

A THESIS SUBMITTED TO
THE FACULTY OF ARCHITECTURE AND ENGINEERING
OF
EPOKA UNIVERSITY

BY

MARVI SHKREPA

IN PARTIAL FULFILLMENT OF THE REQUIREMENTS
FOR
THE DEGREE OF MASTER OF SCIENCE
IN
CIVIL ENGINEERING

JULY, 2023

Approval sheet of the Thesis

This is to certify that we have read this thesis entitled **"Assessing Embankment Dam Slope Stability, Pore Pressure, Reservoir Emptying And Earthquake-Induced Stresses: A Case Study"** and that in our opinion it is fully adequate, in scope and quality, as a thesis for the degree of Master of Science.

_____

Assoc. Prof. Dr. Mirjam Ndini
Head of Department
Date: July, 04, 2023

Examining Committee Members:

Assoc. Prof. Dr. Mirjam Ndini	(Civil Engineering)	_____
Dr. Begmyrat Kulmedov	(Civil Engineering)	_____
Dr. Marsed Leti	(Civil Engineering)	_____

I hereby declare that all information in this document has been obtained and presented in accordance with academic rules and ethical conduct. I also declare that, as required by these rules and conduct, I have fully cited and referenced all material and results that are not original to this work.

Name Surname: Marvi Shkrepa

Signature: _____

ABSTRACT

ASSESSING EMBANKMENT DAM SLOPE STABILITY, PORE PRESSURE, RESERVOIR EMPTYING AND EARTHQUAKE-INDUCED STRESSES: A CASE STUDY

Shkrepa, Marvi

M.Sc., Department of Civil Engineering

Supervisor: Assoc. Prof. Dr. Mirjam Ndini

This thesis focuses on a thorough examination of the stability of dam slopes under a variety of difficult conditions, including pore pressure, abrupt reservoir emptying, and additional stresses brought on by external forces during earthquakes. This thesis's main goal is to investigate the behaviour and stability of embankment dam slopes by thoroughly examining the complex interactions between these variables. The thesis examines the effects of pore pressure, abrupt changes in water level, and earthquake-induced stresses on dam slope stability by utilizing cutting-edge computational algorithms and geotechnical analysis methodologies. The findings of this analysis provide a thorough understanding of potential failure mechanisms and offer insightful advice for the construction and upkeep of dams located in earthquake-prone areas.

Keywords: *Dam, Slope, Stability, Pore Pressure, Failure, Stresses, Earthquake, Geotechnical*

ABSTRAKT

VLERËSIMI I QËNDRUESHMËRISË SË DIGËS, PRESIONI I POREVE, SHKARKIMI I REZERVUARIT DHE SFROCIMET E NXITURA NGA TËRMETET: NJË RAST STUDIMI

Shkrepa, Marvi

Master Shkencor, Departamenti i Inxhinierisë së Ndërtimit

Udhëheqësi: Assoc. Prof. Dr. Mirjam Ndini

Ky studim paraqet analizen e qëndrueshmërisë së digave duke marrë parasysh kushte të ndryshme, përfshirë presionin e poreve, zbrazjen e papritur të rezervuarit dhe sforcimet shtesë që ndodhin nga forcat e jashtme gjatë tërmeteve. Objektivi kryesor i këtij studimi është të analizojë sjelljen dhe stabilitetin e digave me material vendi duke investiguar në mënyrë të gjerë ndërveprimin kompleks midis këtyre faktorëve. Duke përdorur metoda numerike të avancuara dhe teknika analitike gjeoteknike, studimi shqyrton ndikimet e presionit të poreve, ndryshimet e papritura të nivelit të ujit dhe sforcimet që shkaktohen nga tërmetet në qëndrueshmërinë e digave. Rezultatet e kësaj teze ofrojnë njohuri të thella në lidhje me mekanizmat potencialë të dëmtimit dhe sigurojnë perspektiva të vlefshme për projektimin dhe mirëmbajtjen e digave të vendosura në rajone me rrezik ndaj tërmeteve.

Fjalët kyçe: *Diga, Skarpata, Stabiliteti, Presioni i poreve, Dështim, Sforcim, Termet, Gjeoteknikë*

ACKNOWLEDGEMENTS

I would like to thank Assoc. Prof. Dr. Mirjam Ndini, which helped and guided me in conducting this thesis as my Master Thesis Supervisor.

I would like to thank Ing. Arjan Jovani, which helped me with the original construction project of Cerkeze Dam, the geological report, the seismic hazard report and also helped me with the program GeoStudio 12.

TABLE OF CONTENTS

LIST OF TABLES

LIST OF FIGURES

CHAPTER 1

INTRODUCTION

1.1 Problem Statement

Dams are important pieces of infrastructure that offer many advantages, including flood control, irrigation, and the production of hydropower. However, the failure of a dam can have disastrous effects, including the loss of life and damage to property. For instance, the fall of the Banqiao dam in China in 1975 [1] resulted in the deaths of almost 171,000 people and the eviction of millions of people. Given the potentially catastrophic repercussions of dam breakdowns, the analysis of dam stability has recently become a vital topic on a global scale.

Dams are classified into categories depending on their shape and the material which is used to construct them. Widely used are Reinforced Concrete, Steel Dams, Masonry, Buttress and Embankment Dam. In Albania there are 351 dams constructed throughout the years, where a large number of them are embankment dams [2].

1.2 Thesis Objective

One of the main causes of dam slope failure, which results in decreased shear strength and instability, is pore pressure. Rapid changes in the reservoir's water level can cause an imbalance in the hydraulic pressure between the water and the dam's construction, which can lead to the formation of pores in a dam's slope. The shifting soil particles as a result of the increasing pressure could lead to instability and eventual failure. Furthermore, unexpected reservoir emptying, outside forces brought on by earthquakes, and other relevant factors may make the issue worse.

Therefore, it is essential to conduct thorough stability analyses, which is composed of static and dynamic analysis of dam slopes in order to pinpoint potential failure modes and guarantee the security and integrity of dams. In a stability analysis, the stability of the slope and the corresponding safety factor are evaluated in order to determine the stability of a dam. The safety factor is the proportion of driving forces to resisting forces acting on the slope of the dam.

1.3 Scope of work

This thesis presents a comprehensive analysis of the static and dynamic stability of an embankment dam (Cerkeze Dam, Zall Herr, Tirana) constructed with local materials, including an assessment of the deformation curve in the dam body, the stresses induced by hydrostatic pressure, and additional forces resulting from external seismic actions. The evaluation of slope stability will also be examined in this report. The analysis of static and dynamic stability will be conducted in different physical and mechanical conditions, following the subsequent stages outlined below:

1) Analysis of the deformation curve and assessment of pore pressure in the dam foundation using the steady state theory with the method of flow in saturated and unsaturated porous media, known as Darcy's Law.
2) Static analysis and evaluation of effective stresses using the linear equivalent model based on hydrostatic forces.
3) Evaluation of the safety coefficient for slopes using the equilibrium theory with parameter equivalence in Mohr-Coulomb theory.
4) Dynamic analysis and assessment of additional stresses and total stresses due to seismic actions at the base of the dam.
5) Assessment of deformations/displacements and critical failure surface in the dynamic analysis.

CHAPTER 2

LITERATURE REVIEW

2.1 Introduction

The literature used to conduct this thesis is a combination of sever articles, which explain and introduce the reader about types of dams related to the material used in constructing them (reinforced concrete, steel, masonry, rock, etc.). Our focus are enbankment dams that are constructed using material found in the construction site. In order to ensure the safety of the dam over the years, it is necessary to conduct a stability analyses, which consists of static and dynamic. To do so, engineers and researches refer to the standard codes for design (Eurocodes). To analyse the methodology used for making a stability analyses, 5 different articles are provided below, which inform the user mainly about the embankment dams, their construction, design properties etc., and 3 manuals for designing these dams.

2.2 First Article

The author Ubani Obinna has written the article titled 'Earth Dams: Types, construction and modes of failure' [3] that provides an overview of earth dams, including their types, construction, and potential failure modes. It explains that earth dams are structures constructed by compacting soil and rocks to form a barrier that retains water. The different types of earth dams, such as homogeneous earth dams, zoned earth dams, and filter zoned earth dams, are described, and the article highlights the advantages and disadvantages of each type. It also discusses the different construction methods and materials used for earth dams, including compacted earth fill, rolled earth fill, hydraulic fill, and rock fill. Additionally, the potential failure modes of earth dams, such as overtopping, piping, and slope instability, are explained in detail. The article emphasizes the importance of regular inspection and maintenance to ensure the safety and integrity of earth dams. Finally, the article provides a case

thesis of the 1976 Teton Dam failure, which resulted in significant damage and loss of life, highlighting the importance of proper design, construction, and maintenance of earth dams.

2.3 Second Article

The second article written by Anna University's council [4] provides information about the different types of earth dams. It explains that an earth dam is a type of dam constructed using natural materials such as soil, rocks, and clay. The different types of earth dams include homogeneous earth dams, zoned earth dams, and filter zoned earth dams. The article describes the construction of each type of earth dam and their advantages and disadvantages. Homogeneous earth dams are made of uniform soil, while zoned earth dams have different layers of soil with varying properties. Filter zoned earth dams have a filter layer that prevents water from seeping through the dam. It also highlights the importance of proper design and construction of earth dams to ensure their stability and safety. Finally, the article provides examples of notable earth dams worldwide, including the Hoover Dam in the United States and the Tarbela Dam in Pakistan [4].

2.4 Third Article

The author Dirk Van Zyl explains in its lectures about dams that embankment dams are structures built by compacting soil, rock, or other materials to create a barrier that can retain water [5]. The lecture discusses the different types of embankment dams, such as earth fill dams, rockfill dams, and composite dams, and explains their construction and advantages and disadvantages. Earth fill dams are constructed using compacted earth, while rockfill dams are constructed using compacted rock. Composite dams are a combination of earth fill and rockfill dams. The lecture also discusses the factors that affect the stability of embankment dams, such as foundation conditions, seepage, and slope stability. Finally, the lecture highlights the importance

of proper design, construction, and maintenance of embankment dams to ensure their safety and stability [5].

2.5 Fourth Article

The "Manual on Small Earth Dams: A Guide to Siting, Design, and Construction", written by Tim Stephens [6], offers comprehensive guidance on the planning, design, and construction of small earth dams. It covers important aspects such as site selection, dam types, spillway design, embankment stability, seepage control, construction practices, and quality control. The manual emphasizes the significance of proper siting, design, and maintenance for the safety and long-term performance of small earth dams. It serves as a valuable resource for engineers, technicians, and project managers involved in small dam projects, providing them with detailed guidelines to ensure successful implementation while prioritizing safety and sustainability [6].

2.6 Fifth Article

This article written by Amjad Hussain Bhutto [7] explains in depth the stability of embankment dams under static loading (Bhutto, 2020). It begins by explaining a cross-section model of an embankment dam, the method used to calculate mathematically static stability, soil conditions, types of failure and boundary conditions. By also using software applications it determines modes of failure (graphically explained), weakened areas and static stability check. The programme itself uses FEM (Finite Element Method) to mathematically operate and give the required results for each failure mode [7].

2.7 Design Standards

Design Standards No. 13, specifically Chapter 2 on Embankment Dams [8], focuses on the final phase of embankment design, emphasizing hydraulic structures. This chapter provides detailed guidelines for the design, construction, and maintenance of hydraulic structures within embankment dams. It covers important aspects such as spillways, outlet works, and control structures, emphasizing the need for proper design to ensure the efficient and safe functioning of these structures. The standards outlined in this chapter serve as a valuable resource for engineers and professionals involved in the design and implementation of embankment dams, promoting best practices and ensuring the long-term stability and performance of these hydraulic structures [8].

2.8 Eurocode 7 & 8

Eurocode 7 is a European standard that provides guidelines for the design of geotechnical structures and foundations [9]. It aims to ensure the safety, serviceability, and durability of geotechnical works by considering the principles of soil mechanics and geotechnical engineering. Eurocode 7 covers various aspects, including site investigation, design parameters, analysis methods, and verification procedures for stability and settlement calculations. It also addresses geotechnical aspects of retaining structures, slopes, and foundations. Eurocode 7 is widely adopted by European countries as a common set of design rules and is an essential reference for geotechnical engineers involved in the design and construction of structures in Europe [9].

Eurocode 8 is a European standard that provides guidelines for designing structures to resist earthquake forces [10]. It aims to ensure the safety and stability of buildings and civil engineering works during seismic events. Eurocode 8 covers various aspects, including seismic hazard assessment, ground motion characterization, structural analysis and design, and detailing requirements for different types of structures. It provides procedures for determining seismic actions, calculating seismic forces, and designing structures to resist these forces. Eurocode 8 is widely adopted in

European countries as a reference for seismic design and is an important tool for engineers involved in the design and construction of earthquake-resistant structures in Europe [10].

CHAPTER 3

METHODOLOGY

3.1 Outline of the dam characteristics

The Çerkezë Reservoir is located in the village of Çerkezë, Zall-Herr Administrative Unit, Municipality of Tirana, in the northern part of the Kamëz Municipality, with an area of 616,000 m^2. The storage capacity of the reservoir, as per the project, was 4,800,000 m^3 and it has an irrigation capacity of approximately 300 hectares. This reservoir was constructed in 1968 using local materials such as gravel and clay. The area where the Çerkezë Reservoir is situated is part of the TRU-1-4 water scheme, which extends along the Çerkezë valley for about 3-4 km in the middle stream. Over the years, the embankment of this reservoir has experienced stability issues, with ongoing gradual slope failures despite the water level reduction. Currently, the upper slope of the embankment near the discharge channel exhibits slip zones and erosion in the lower part of the reservoir due to water pressure. One of the main causes could be the malfunctioning of the drainage system within the embankment. Overall, the condition of this reservoir is characterized by damages to the internal slope, posing a risk to the residents in the urban areas located downstream of the embankment. The reservoir was created by the construction of the Çerkezë Dam, which incorporates a non-pressurized type of spillway in its structure, as well as a catastrophic discharge channel.

Figure 1. Geographic location of Dam

The Çerkezë Dam is constructed using local materials, with a homogeneous structure composed of clayey soil. According to the ICOLD recommendations [2], the dam height is 24 meters, and the crest elevation is 99.0 m, while the crest length is 250 meters. The final elevation of the dam is 75 m. The normal water level in the reservoir is at an elevation of 95 m, with a projected volume of approximately 4,800,000.00 m^3. However, the current measured water volume at this level, as of 2022, is 3.8 million m^3. The dam has a homogeneous cross-section with a crest width of 3.5 m and side slopes with a slope ratio of 1:2.5 in the upper part of both slopes.

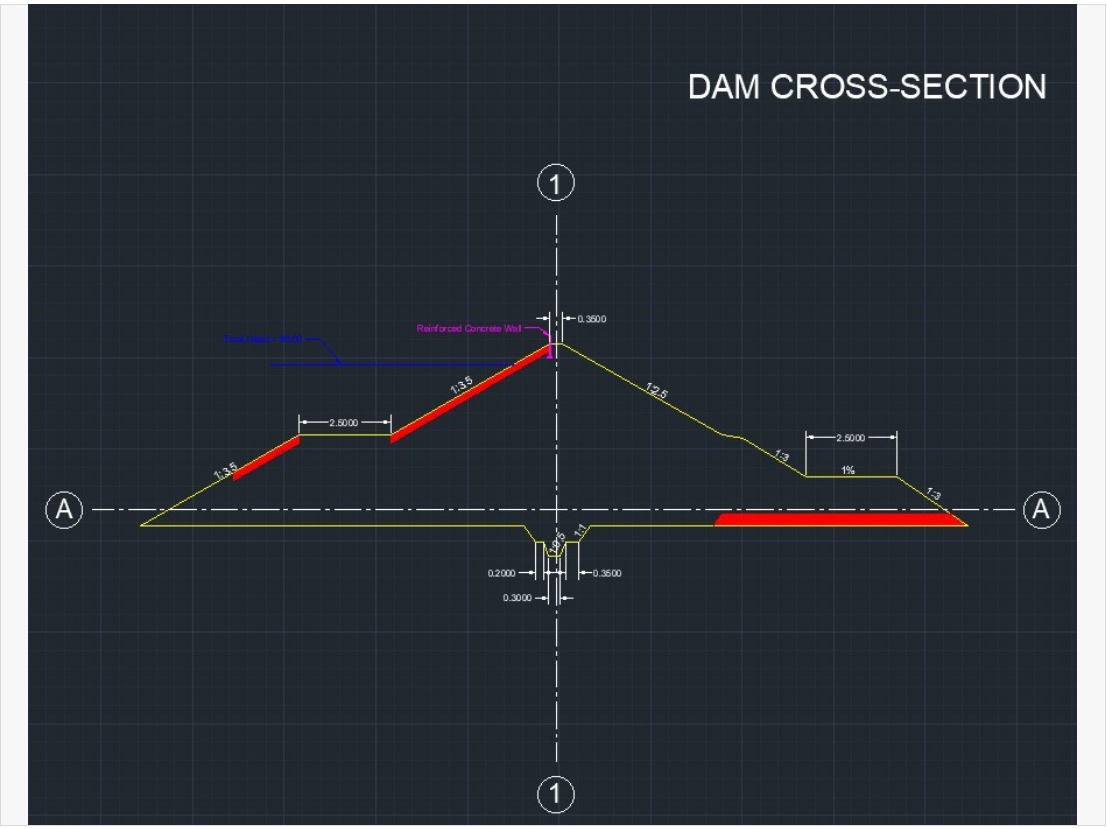

Figure 2. Dam cross-section from original project

At elevation 91.75 m on the upstream side of the dam, there is a berm with a width of 25 m, and on the downstream side, there is a berm with a width of 6 m. The coefficient of permeability of the clayey soil is 1.2x10-7 (cm/s). The clayey foundation is covered on both sides with filter layers that extend to the foundation level to serve as drainage. The slope ratio of the dam in its upper part, both on the upstream and downstream sides, is 1V:2.5H, while in the lower part of the upstream side, it is 1:3.5 m, and on the downstream side, it is 1V:3.0H.

3.2 Geological report

The geological-engineering conditions thesis for the Çerkezë Dam in Fushe Kruje, Administrative Unit Zall-Herr, Municipality of Tirana, for the implementation phase, has developed a detailed program as follows:

The main works carried out to assess the characteristics of this landslide are:

- Geological survey of the landslide zone, limiting the sliding body using topographic measurements.
- Topographic and geological-engineering mapping and cross-sections have been prepared.
- Excavations at the sliding zone with depths of 6.0 m, 7.0 m, and 10.00 m.
- Collection of samples with disturbed and undisturbed structures.
- Laboratory analyses.
- Preparation of geological and geotechnical reports with respective recommendations.

Physical-Geological and Geodynamic Processes: In thesising the geological phenomena in this area, we have relied on existing studies and the new information obtained from the current thesis. Based on these data, we describe the geological phenomena present in the geological formations encountered in this area.

The most notable geological and geodynamic phenomena observed in this area are:

- Land sliding phenomenon
- Erosion phenomenon
- Movement of diluvial-eluvial cover towards the relief descent.

These phenomena are explained in detail in the Geotechnical-Geological report, which identified four layers, including the dam body, and provided the characteristics/parameters for each of them. The parameter values were obtained from laboratory testing on samples.

3.2.2 Layer No. 1

Represented by: Vegetal and herbaceous soil, medium to fine-grained, brownish with dark and black spots, moist, and plastic. They contain plant roots and are loosely compacted.

3.2.3 Layer No. 2

Represented by: Medium to light clayey soil, brownish to coffee-colored, with gray lenses, moist, and in a plastic state. They contain thin layers of sand and a few gravels. They are moderately compacted. The physical-mechanical characteristics for this layer are:

Table 1. Physical & Mechanical properties of Layer no. 2

Granulometric composition:
Clay fraction < 0.002 mm: 34.8%
Silt fraction 0.002-0.075 mm: 37.6%
Sand fraction > 0.075 mm: 21.1%
Gravel fraction > 4.75 mm: 6.50%
Plasticity:
Upper plasticity limit Wrr = 42.70%
Lower plasticity limit Wp = 22.6%
Plasticity index F = 20.1
Natural moisture content Wn = 24.5%
Specific weight δ = 2.68 T/m^3
Bulk unit weight in natural state Δ = 1.98 T/m^3
Porosity coefficient ε = 0.7
Deformation modulus E = 98 kg/cm^2
Internal friction angle ϕ = 19o
Cohesion C = 0.29 kg/cm^2
Other parameters:

Internal friction angle ϕ = 10 degree
Cohesion C = 0.07 kg/cm^2
Allowable compression stress σ = 1.80 kg/cm^2

3.2.4 Layer No. 3

Represented by: Argillites, aleurolites, and shales, with a brownish, gray, and coffee-colored appearance. They have a lower moisture content, with weak to moderate cementation. They contain thin clayey layers. The physical-mechanical characteristics for this layer are:

Table 2. Physical & Mechanical properties of Layer no. 3

Granulometric composition:
Clay fraction < 0.002 mm: 39.6%
Silt fraction 0.002-0.075 mm: 35.70%
Sand fraction > 0.075 mm: 19.5%
Gravel fraction > 4.75 mm: 5.20%
Plasticity:
Upper plasticity limit Wrr = 42.9%
Lower plasticity limit Wp = 21.3%
Plasticity index F = 21.6
Natural moisture content Wn = 11.9%
Specific weight δ = 2.6 T/m^3
Bulk unit weight in natural state Δ = 2.23 T/m^3
Deformation modulus E = 692 kg/cm^2
Internal friction angle ϕ = 29.6o
Cohesion C = 0.48 kg/cm^2
Allowable compression stress σ = 2.80 kg/cm^2

Compression strength uniaxial Rsh = 16.8 kg/cm^2

3.2.5 Layer No. 4

Represented by: Argillites, shales, and aleurolites, gray in color, with lower moisture content, ranging from moderate to good cementation, and exhibiting fissures. They contain thin clayey layers. They are highly compacted. The physical-mechanical characteristics for this layer are:

Table 3. Physical & Mechanical properties of Layer no. 4

Natural moisture content Wn = 5.9%
Bulk unit weight in natural state Δ = 2.37 T/m^3
Internal friction angle ϕ = 30.8o
Cohesion C = 0.62 kPa
Compression strength uniaxial Rsh = 28.4 kg/cm^2
Deformation modulus E = 987 kg/cm^2
Allowable compression stress σ = 3.5 kg/cm^2

3.3 Seismic hazard report

The experts from the consulting firm conducted a seismic risk assessment that could threaten this construction site in rocky soil conditions using a contemporary probabilistic methodology known as Cornell-McGuire.

The seismic risk assessment of the site under specific and concrete conditions was performed based on similar studies and assessments in the area, utilizing the computer program "SHAKE 2000".

Seismic risk was expressed through the physical parameters of ground shaking resulting from earthquake vibrations, such as the maximum peak ground acceleration (PGA) and spectral accelerations (SA) for the periods of ground motion.

From the perspective of the soil layers constituting the construction site, it is classified as category II soil according to the Albanian Design Code KTP-N.2-89 and based on the average shear wave velocity for the entire depth Vs30=426.36 m/s, it is classified as class "B" soil according to Eurocode.

The seismic risk assessment of the construction site was conducted using the probabilistic Cornell-McGuire method. The values of maximum ground motion velocity (PGA) were calculated for rocky soil, considering a 10% exceedance probability in 50 years and a 10% exceedance probability in 10 years (exposure time and economic life), corresponding to return periods of earthquakes of 95 and 475 years, in full compliance with Eurocode 8. Thus, based on the seismic risk calculations for the considered construction site, the PGA values are 0.142 g for rocky soil conditions and a 10%/10-year probability, and 0.291 g for a 10%/50-year probability.

Table 4. Return Period & PGA (Peak Ground Acceleration)

Return Period	**PGA**
95 years	0.142 g
475 years	0.291 g

Response Spectra of Strong Ground Motion From the analyses performed using the "SHAKE 2000" program to assess the response to strong ground motions for each construction site, response spectra for acceleration, velocity, and Fourier amplitude spectrum amplification are typically determined.

Here, we will focus only on the response spectrum of acceleration, which is an important parameter for each construction site. The acceleration response spectra are presented for 5% damping in spectral acceleration values, for each accelerogram or all used accelerograms, at different levels of the construction site.

Thus, for our case thesis, the maximum response of the geotechnical model of the construction site is calculated at the layer 1 level on the surface of this site, under the action of an earthquake with return periods of 95 and 475 years.

Vibration Periods of the Ground An important parameter for the dynamic response of the soil is the vibration periods of the rock layers deposited on the bedrock.

The predominant period of ground vibration at the construction site can be calculated using the formula TP = 4H/ V, where TP is the predominant period, H is the thickness of the deposit layer, and V is the shear wave velocity. For example, TP = 4 x 8.2 / 240 = 0.136 seconds.

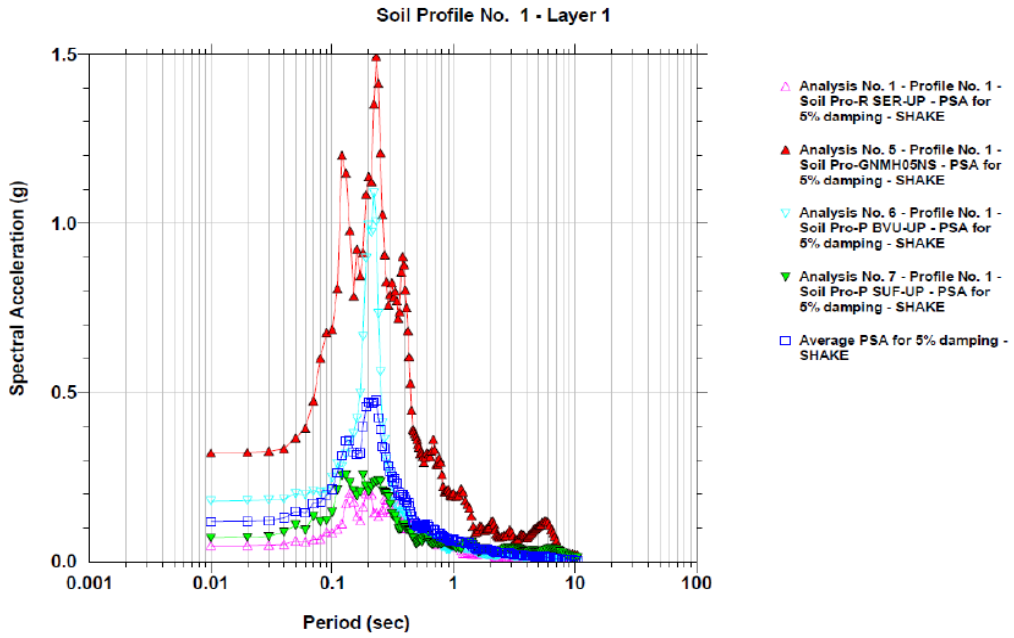

Figure 3. Spectral Analysis of Excitation Response at Layer 1 for a 95-Year Repetition Period, calculated for six input functions and their average value

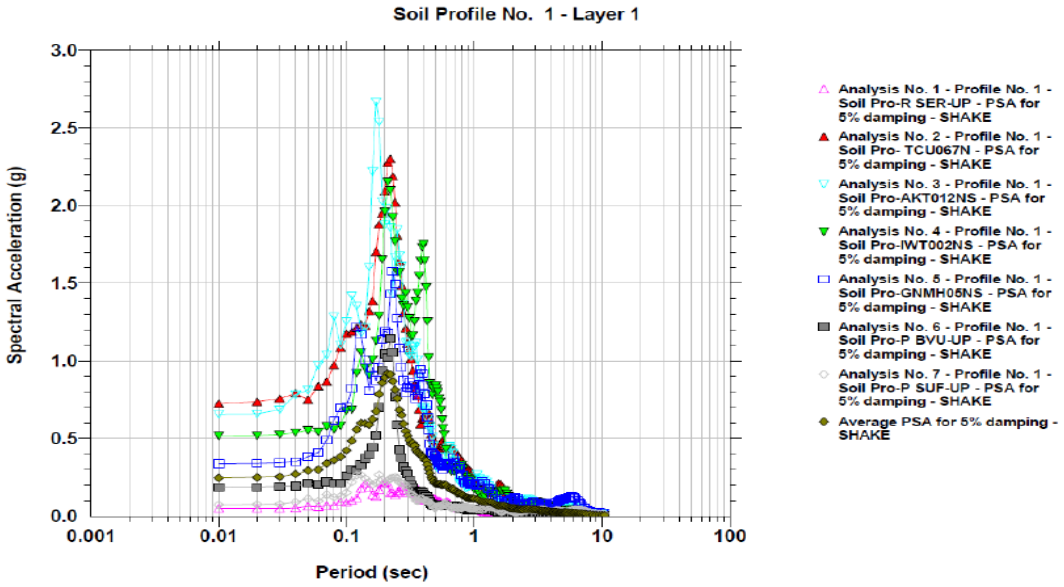

Figure 4. Spectral Analysis of Excitation Response at Layer 1 for a 475-Year Repetition Period, calculated for six input functions and their average value

3.4 GeoStudio 12

GeoStudio 12 is a widely utilized, comprehensive software program employed for static and dynamic analysis of dams. It equips engineers and geotechnical professionals with a robust suite of tools to examine the behaviour and stability of dams under diverse loading conditions. The following provides an overview of GeoStudio 12's capabilities and features for dam analysis:

Static Analysis: GeoStudio 12 encompasses robust static analysis capabilities that enable the evaluation of dam stability under static loading conditions. The software facilitates the modelling of dam geometry, including slopes, crest, and foundation, through various built-in modelling tools. Advanced material modelling options, such as linear elastic, Mohr-Coulomb, and Hoek-Brown, are available to accurately represent the behaviour of dam materials. Users can define different boundary conditions, including water pressure, pore pressure, and external loads, to simulate realistic scenarios. GeoStudio 12 employs sophisticated numerical methods, notably the finite element method, to solve governing equations and compute the factor of safety and stability analysis results. The software offers visualization tools to generate contour plots, stress/strain diagrams, and displacement profiles, aiding in comprehensive understanding of dam behaviour.

Dynamic Analysis: GeoStudio 12 incorporates dynamic analysis capabilities for assessing the response of dams to seismic events and other dynamic loads. The program utilizes the spectral method to compute the dynamic response of the dam system. Users can model dynamic excitation using earthquake records or custom-defined input functions. GeoStudio 12 allows for the incorporation of dynamic soil properties, such as dynamic modulus and damping, to accurately capture the dynamic behaviour of the dam and its foundation. Both frequency and time domains can be analysed to examine the dynamic effects on the dam's response, enabling detailed investigations. Engineers can evaluate dam stability and potential liquefaction zones by considering computed pore water pressure and shear strength parameters. The software facilitates the assessment of displacement and stress distributions during dynamic loading, aiding in dam structure design and reinforcement.

In summary, GeoStudio 12 is a versatile software package offering powerful static and dynamic analysis capabilities for comprehensive dam analysis. It supports engineers in evaluating dam stability, safety, and performance under various loading conditions, enabling informed decision-making and the design of reliable and resilient dam structures.

3.5 Mathematical analysis

For the analysis of slope stability, reinforced conditions, and deformations, the engineering program GeoStudio has been used, which is a specialized engineering program for mathematical analysis of geotechnical problems.

The fundamental basis of the engineering program is the FINITE ELEMENT METHOD. For the purpose of mathematical analysis, the model with the finite element method using 2D elements of the slope in "reinforced conditions" will be employed.

The finite element method (FEM) is a numerical approach for solving problems where the numerical field variables are related to a differential equation.

The numerical solution is based on the principle of discretization, where the field is represented by a series of 'finite elements'. Shape functions determine the distribution of the dependent variable within each element. Consequently, the value of the dependent variable anywhere within each element is a function of the dependent variable at the element nodes.

The finite element method (FEM) is a general numerical method for solving partial differential equations in two or three spatial dimensions. To solve a problem, FEM divides a large system into smaller, simpler parts called finite elements. This is achieved through a specific discretization in the spatial dimensions, which is implemented by constructing a mesh of the object that has a limited number of points. The formulation of the finite element method for a boundary value problem ultimately results in a system of algebraic equations. The simple equations that model these finite elements are then assembled into a larger system of equations that models the entire

problem. The finite element method subsequently approximates a solution by minimizing an associated error function through variation calculations.

3.6 Depression curve

By definition the depression curve is the change in water elevation from the upstream of the embankment dam to the downstream section. It is strongly influenced by several factors including the dam's geometry, hydraulic characteristics of the basin and the downstream river.

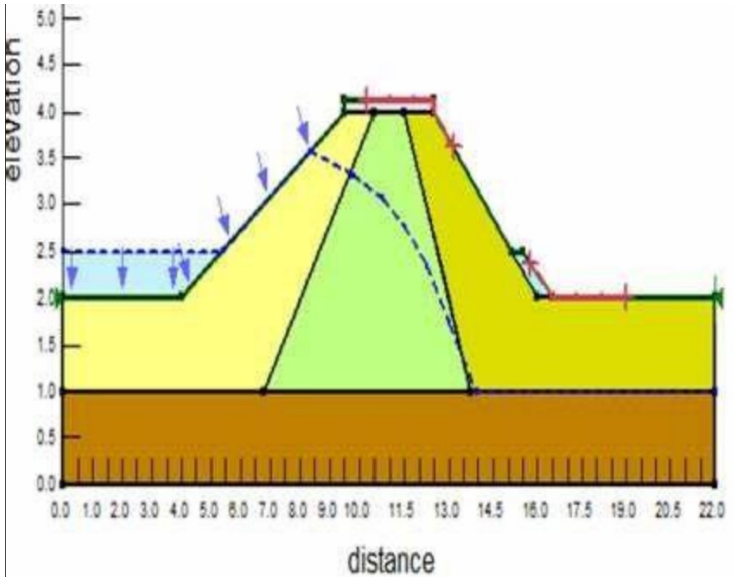

Figure 5. Simple model of depression curve

The depression curve is based on the laws of mass and energy conservation. This law is applied to the nodes of the finite element, which must satisfy two conditions:

1) The total volume entering each node is equal to the volume exiting the node plus the difference in volume storage (the rate of change of water vapor).
2) Energy losses in the finite element system must be balanced at each node of the system.

$$\boldsymbol{Mst = \frac{dMst}{dt} = \mathrm{m(in)} - m(out) + Ms} \qquad (\boldsymbol{Equation\ 1})$$

Where:

Mst - represents the stored mass or volume;

m(in) – m(out) represents the mass of water transported from one element to another;

Ms - represents the rate of change of water vapor.

The above equation, expressed in a simplified form, is given as follows:

$$\boldsymbol{Mst = Mw + Mv} \qquad (\boldsymbol{Equation\ 2})$$

Where:

Mst - represents the stored mass or volume;

Mw - represents the rate of change of water volume;

Mv - represents the rate of change of water vapor.

The rate of change of water volume from one element to another during the Finite Element Method (FEM) analysis is dependent on several parameters related to the equation as follows:

$$\boldsymbol{Mw = \rho w\left(\theta w \beta w \frac{\partial uw}{\partial t} + \beta \frac{\partial uw}{\partial t} + mw \frac{\partial \varphi}{\partial t}\right) + \theta w \rho w \alpha w \frac{\partial T}{\partial t}} \quad (\boldsymbol{Equation\ 3})$$

Where:

ρw - represents the density of water;

θw - represents the volumetric content of water;

βw - represents the isothermal compressibility of water;

uw - represents the pore pressure of water;

β - represents the bulk compressibility of the soil;

mw - represents the porosity function gradient of water content;

αw - represents the coefficient of thermal expansion at constant pressure of water;

($\varphi = ua - uw$) - represents the difference between air pore pressure and water pore pressure.

It should be noted that in saturated soils, the bulk compressibility is a function of the relative change in volume (K, bulk modulus), thus β = 1/K.

The relative change in volume of the soil is determined by the parameters of the elastic modulus (E) and the Poisson's ratio (μ) in two-dimensional planes with the formula:

$$\boldsymbol{K = \frac{E}{[(1 + \mu)(1 - 2\mu)]}} \qquad (\boldsymbol{Equation\ 4})$$

The rate of change of water vapor from one element to another during the Finite Element Method (FEM) analysis is dependent on several parameters related to the equation as follows:

$$\boldsymbol{Mv = \frac{\partial Mv}{\partial t} = \frac{M}{R}\frac{\partial}{\partial t}\left(\frac{\rho v Va}{T}\right) = \frac{M}{R}\frac{\partial}{\partial t}\left(\frac{\rho v \theta a}{T}\right) dxdydz} \qquad (\boldsymbol{Equation\ 5})$$

Where:

M - represents the molar mass;

R - represents the gas constant (8.314472 J·K−1·mol−1);

ρv - represents the vapor pressure;

Va - represents the volumetric content of air.

The rate of water flow from one element to another, based on the law of mechanical energy according to Darcy's law, is expressed as follows:

$$mw = \rho wqwdxdz = \frac{-Kw}{g}\left(\frac{\partial uw}{\partial y} + \rho wg\frac{\partial y}{\partial y}\right)dxdz \qquad (Equation\ 6)$$

Where:

qw - represents the volume flux of water;

Kw - represents the hydraulic conductivity of water.

The rate of vapor flow of water from one element to another, based on the law of mechanical energy according to Fick's law, is expressed as follows:

$$mv = -Dv\frac{\partial \rho v}{\partial y}dxdz \qquad (Equation\ 7)$$

Where:

Dv - represents the diffusion coefficient of water vapor in the soil materials.

The calculation of the depression curve will also take into account the case of immediate drawdown of the water level in the upper reservoir of the dam.

The consideration of water level movement from the maximum level to the minimum level over time, which will be determined by the discharge capacity of the intake works in the water supply system, will analyse the upper slope with a lower resistance of the dam body.

According to the theory of soil mechanics, soils are called semi-saturated when they are above the water table, and pore pressure has a negative sign. The negative pore pressure is related to the pressure developed within soil particles, which is smaller than the atmospheric pressure.

Negative pore pressure reaches its maximum value when the capillary movement of water within the soil body is almost stagnant (v=0 m/s). The movement of water within the soil body depends on the hydraulic conductivity parameter.

The higher the hydraulic conductivity in the soil body, the faster the maximum value of material resistance is reached as the water level decreases.

To explain the case that will occur for the considered dam, even though the water level in the upper slope will decrease, the pore pressure remains positive. This means that the resistance of the material in the upper slope will decrease, and as a result, its stability will decrease.

The main reason is the hydraulic conductivity parameter, which in dams with clay materials in their body has a very small hydraulic conductivity, which means that even in a very short time of immediate drawdown of the water level, the pore pressure will remain positive.

This implies that the effective stresses in the upper slope will be smaller, and as a result, its resistance will be lower, which will jeopardize its stability.

The effective stresses can be expressed as follows:

$$\boldsymbol{\sigma v' = \sigma - u} \qquad (\boldsymbol{Equation\ 8})$$

where u represents the pore water pressure.

$$\boldsymbol{\sigma v' = Hdh * \gamma dh - Hwater * \gamma water} \qquad (\boldsymbol{Equation\ 9})$$

When the water level is drawn down, the air pressure remains the same as the height of the soil Hdh = Hwater:

$$\boldsymbol{\sigma v' = Hdh * (\gamma dh - \gamma water)} \qquad (\boldsymbol{Equation\ 10})$$

To perform a mathematical modelling with a transient method where variables change with time, it is necessary to calculate the time of reservoir discharge from the hydraulic structure of the water supply system.

Reservoir Volume → V=4,550,000m^3

Water Level Height: → H=14m

Water Surface Area: → a=2.25m^2

Discharge Coefficient: → Cd=0.67

Average Reservoir Surface Area → A=V/H=4,550,000/14=325,000.0m^2

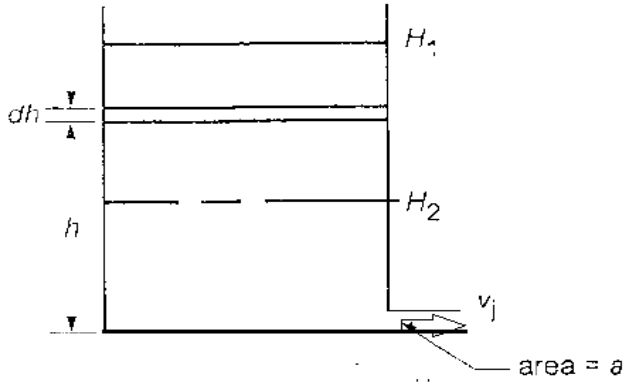

Figure 6. Dam water emptying model

The Bernoulli's equation at the water surface determines the pressure P1, and at the discharge point determines the pressure P2. From the equality P1=P2, the velocity of water discharge is determined as v=(2*g*H)^0.5.

From the decrease in water level by a depth delta H (dH) over a time interval delta t (dt), we determine the change in volume at each point: at point P1, located at the water surface, V1=A**dH, while at the discharge point where the pressure is P2, we determine V2=Q2**dt, where Q2= Cd**a** *v*= *Cd***a*(2*g*H)^0.5.

The final equation is:

$$-A \times dH = Cd \times a\sqrt{2 \times g \times H} \times dt \qquad (Equation\ 11)$$

$$T = \int dt = \int_{H}^{H^2} \frac{A \times dH}{Cd \times a\sqrt{2 \times g \times H}} \qquad (Equation\ 12)$$

$$T = \frac{2A}{Cd \times a\sqrt{2 \times g}}\left(\sqrt{H1} - \sqrt{H2}\right) \qquad (Equation\ 13)$$

For the water level H2=0, the time T is sought, and the formula is applied:

$$T = \frac{2A}{Cd \times a\sqrt{2 \times g}} \times \sqrt{H1} \qquad (Equation\ 14)$$

3.7 Reinforced Slope

The method used for the analysis of the reinforced slope and its safety factor is based on the overall limit equilibrium principle. This method relies on two equations that determine the safety factor. The first equation ensures force equilibrium, while the second equation ensures moment equilibrium.

The safety factor, obtained from the above equations, is defined as the factor by which the cutting force of the soil decreases in order for the mass of the soil to reach a limited equilibrium state along a selected surface or slope.

For an analysis of effective stresses, the cutting force is given by the Mohr-Coulomb formula:

$$\tau = c' + (\sigma n - u) \times \tan \varphi' \qquad (Equation\ 15)$$

Where:

τ = cutting force;

c’ = effective cohesion;

φ’ = effective internal friction angle;

σn = total normal stresses;

u = pore water pressure.

The stability analysis is based on a specific radius slope, divided into several vertical blocks with a defined thickness.

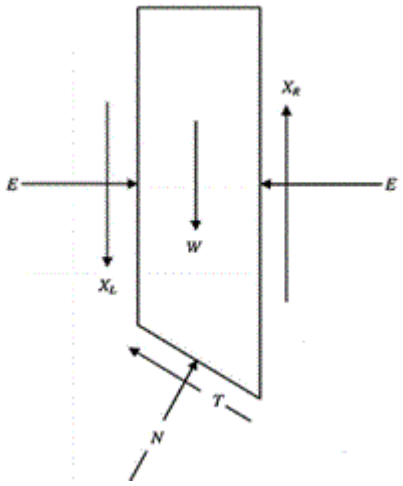

Figure 7. Blockade forces in the reinforced sector

XR = right vertical shear force;

XL = left vertical shear force;

E = normal shear force;

N = block base normal force;

T = block base shear force;

W = weight of the block.

The General Limit Equilibrium (GLE) method uses static equations to solve for the factor of safety:

- The sum of vertical cutting forces for each block to determine the normal force in the failed slope (N).
- The sum of horizontal normal forces for each block to determine the normal force between two blocks (E).
- The sum of moments at a common point to determine the moment equilibrium (Fm).
- The sum of horizontal forces for all blocks to determine the force equilibrium (Ff).

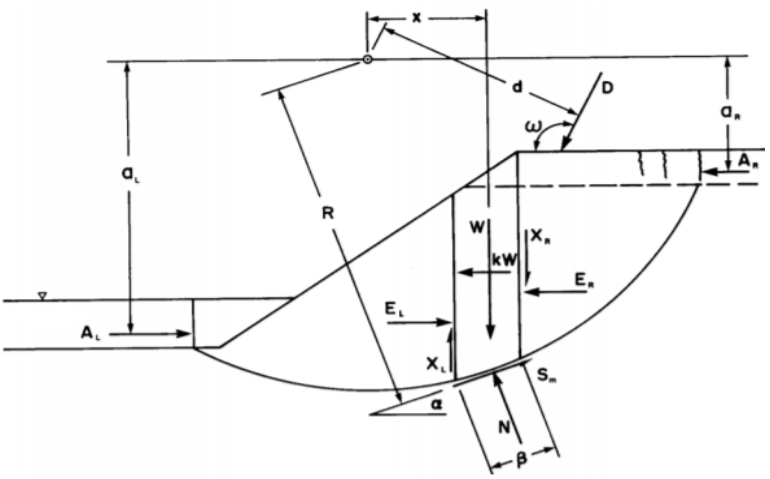

Figure 8. Blockade forces in the reinforced sector based on the equations

$$\sum \boldsymbol{Wx} - \sum \boldsymbol{SmR} - \sum \boldsymbol{Nf} + \sum \boldsymbol{kWe} \pm \sum \boldsymbol{Dd} \pm \sum \boldsymbol{Aa} = \mathbf{0} \quad (\boldsymbol{Equation}\ \mathbf{16})$$

$$\boldsymbol{Fm} = \frac{\sum((\boldsymbol{c'\beta R} + (\boldsymbol{N} - \boldsymbol{u\beta})\boldsymbol{R}\ \boldsymbol{tan}\ \emptyset'))}{\sum \boldsymbol{Wx} - \sum \boldsymbol{Nf} \pm \sum \boldsymbol{Dd}} \quad (\boldsymbol{Equation}\ \mathbf{17})$$

$$\sum(\boldsymbol{EL} - \boldsymbol{ER}) - \sum(\boldsymbol{N}\ \boldsymbol{sin}\ \boldsymbol{\alpha}) + \sum(\boldsymbol{Sm}\ \boldsymbol{cos}\ \boldsymbol{\alpha}) - \sum(\boldsymbol{kW}) + \sum \boldsymbol{D}\ \boldsymbol{cos}\ \boldsymbol{\omega} \pm \sum \boldsymbol{A} = \mathbf{0} \quad (\boldsymbol{Equation}\ \mathbf{18})$$

$$\boldsymbol{Ff} = \frac{\sum[\boldsymbol{c'\beta}\ \boldsymbol{cos}\ \boldsymbol{\alpha} + (\boldsymbol{N} - \boldsymbol{u\beta})\ \boldsymbol{tan}\ \emptyset'\ \boldsymbol{cos}\ \boldsymbol{\alpha}]}{\sum \boldsymbol{N}\ \boldsymbol{sin}\ \boldsymbol{\alpha} - \sum \boldsymbol{D}\ \boldsymbol{cos}\ \boldsymbol{\omega}} \quad (\boldsymbol{Equation}\ \mathbf{19})$$

$$(\boldsymbol{XL} - \boldsymbol{XR}) - \boldsymbol{W} + \boldsymbol{N}\ \boldsymbol{cos}\ \boldsymbol{\alpha} + \boldsymbol{Sm}\ \boldsymbol{sin}\ \boldsymbol{\alpha} - \boldsymbol{D}\ \boldsymbol{sin}\ \boldsymbol{\omega} = \mathbf{0} \quad (\boldsymbol{Equation}\ \mathbf{20})$$

$$\boldsymbol{N} = \frac{\boldsymbol{W} + (\boldsymbol{XR} - \boldsymbol{XL}) - \frac{\boldsymbol{c'\beta}\ \boldsymbol{sin}\ \boldsymbol{\alpha} + \boldsymbol{u\beta}\ \boldsymbol{sin}\ \boldsymbol{\alpha}\ \boldsymbol{tan}\ \emptyset'}{\boldsymbol{F}}}{\boldsymbol{cos}\ \boldsymbol{\alpha} + \frac{\boldsymbol{sin}\ \boldsymbol{\alpha}\ \boldsymbol{tan}\ \emptyset'}{\boldsymbol{F}}} \quad (\boldsymbol{Equation}\ \mathbf{21})$$

c' = effective cohesion;

ϕ' = effective internal friction angle;

u = pore water pressure;

kWe= seismic force;

N = normal force on the sliding plane;

W = weight of the block;

E = normal force on block faces;

X = shear force on block faces;

D = resultant force;

β, R, x, f, d, ω = geometric parameters;

α = block inclination angle.

The factor of safety, which satisfies both moment equilibrium and force equilibrium, is considered to be the convergent factor of safety according to the General Limit Equilibrium method.

As seen from the above equations, the normal force (N) on the sliding plane is a component in both equations. The equations are nonlinear, and for this purpose, the shear forces (XR & XL) will be determined by the Morgenstern and Price (1965) equation:

$$\boldsymbol{X = E * \lambda * f(x)} \qquad (\boldsymbol{Equation\ 22})$$

Where:

λ - represents the percentage of the function used f(x);

f(x) - represents the shear force function that represents the relative direction of the resultant shear force.

3.8 Static and Dynamic Analysis

Analysis of stress/deformation is based on the equations of potential energy and the weighted residuals method. The analysis is performed using a 2D model.

The aim of this analysis is to make quantitative predictions, compare alternatives, identify predominant parameters, and understand the stress/deformation processes.

Static analysis relies on key parameters such as:

- E - Young's modulus
- v - Poisson's ratio
- C - Cohesion
- ϕ - Internal friction angle

The total vertical stresses will be represented according to the following equation:

$$\boldsymbol{\sigma v = \sum_{1}^{n} yi \times zi} \qquad (\boldsymbol{Equation\ 23})$$

Where:

- zi - Thickness of the layer
- yi - Bulk density of the material

In the case of water presence within the soil material, the vertical stresses will be based on effective stresses:

$$\boldsymbol{\sigma v = \sum_{1}^{n} (yi \times zi - u)} \qquad (\boldsymbol{Equation\ 24})$$

Where u is the pore water pressure.

The horizontal stresses will be represented by a coefficient K0, which is related to the Poisson's ratio:

$$\boldsymbol{\sigma' h = K0 \times \sigma' v} \qquad (\boldsymbol{Equation\ 25})$$

$$\boldsymbol{K0 = \frac{\sigma' h}{\sigma' v} = \frac{v'}{1 - v'}} \qquad (\boldsymbol{Equation\ 26})$$

The tensile stresses will be based on Hooke's law:

$$\boldsymbol{E = \frac{\Delta \sigma}{\Delta \varepsilon}\ ;\ \Delta \varepsilon = \frac{\Delta \sigma}{E}} \qquad (\boldsymbol{Equation\ 27})$$

Calculating the effective stresses is crucial for determining the shear strength, which is given by the Mohr-Coulomb formula:

$$\boldsymbol{\tau = c' + (\sigma n - u) \times tan\, \varphi'} \qquad (\boldsymbol{Equation\ 28})$$

Where:

τ - represents the shear strength;

c' - is the effective cohesion;

φ' - is the effective internal friction angle;

σn - is the total normal stresses;

u - is the pore water pressure.

In static analysis, the relationship between compressive and tensile stresses is based on the linear-elastic model:

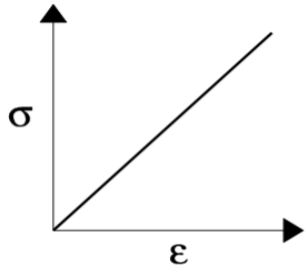

Figure 9. Linear-Elastic Model

The fundamental equation for the relationship between compressive and tensile stresses is given as follows:

$$\begin{Bmatrix} \sigma x \\ \sigma y \\ \sigma z \\ \tau xy \end{Bmatrix} = \frac{E}{(1+v)(1-2v)} \begin{bmatrix} 1-v & v & v & 0 \\ v & 1-v & v & 0 \\ v & v & 1-v & 0 \\ 0 & 0 & 0 & \frac{1-2v}{2} \end{bmatrix} \begin{Bmatrix} \varepsilon x \\ \varepsilon y \\ \varepsilon z \\ \varepsilon xy \end{Bmatrix} \textbf{(Equation 29)}$$

Dynamic analysis is based on the spectral method, where the equation of motion for the dynamic response of a system formulated using the finite element method is given as follows:

$$[\boldsymbol{M}] \times \{\boldsymbol{a1}\} + [\boldsymbol{D}] \times \{\boldsymbol{a2}\} + [\boldsymbol{K}] \times \{\boldsymbol{a3}\} = \{\boldsymbol{F}\} \qquad (\boldsymbol{Equation\ 30})$$

Where:

- [M] is the mass matrix
- [D] is the damping matrix
- [K] is the stiffness matrix
- {F} is the load vector
- {a1 } is the nodal acceleration vector
- {a2} is the nodal velocity vector
- {a3} is the nodal displacement vector

The load vector consists of the self-weight forces of the structure, external forces such as water pressure or floods, and seismic forces.

The mass matrix is a function of density parameter and a diagonal matrix of mass distribution factors.

$$[\boldsymbol{M}] = \int_{\boldsymbol{v}} \boldsymbol{\rho}[\boldsymbol{\varphi}]\boldsymbol{dv} \qquad (\boldsymbol{Equation\ 31})$$

The damping matrix is determined using the following formula:

$$[\boldsymbol{D}] = \boldsymbol{\alpha} \times [\boldsymbol{M}] + \boldsymbol{\beta} \times [\boldsymbol{K}] \qquad (\boldsymbol{Equation\ 32})$$

Where α and β are the Rayleigh damping coefficients, which are related to the damping ratio (η).

$$\boldsymbol{\eta} = \frac{\boldsymbol{\alpha} + \boldsymbol{\beta} \times \boldsymbol{\omega}^2}{\boldsymbol{2\omega}} \qquad (\boldsymbol{Equation\ 33})$$

The stiffness matrix is given by the following formula:

$$[\boldsymbol{K}] = \int_{v} [\boldsymbol{B}]^{\boldsymbol{T}} [\boldsymbol{C}][\boldsymbol{B}]\boldsymbol{dv} \qquad (\boldsymbol{Equation\ 34})$$

Where:

- [B] is the displacement matrix
- [C] is the unit stiffness matrix, which is a function of Young's modulus (E) and Poisson's ratio (ν).

$$[\boldsymbol{C}] = \frac{\boldsymbol{E}}{(\boldsymbol{1}+\boldsymbol{v})(\boldsymbol{1}-\boldsymbol{2v})}\begin{bmatrix} \boldsymbol{1-v} & \boldsymbol{v} & \boldsymbol{v} & \boldsymbol{0} \\ \boldsymbol{v} & \boldsymbol{1-v} & \boldsymbol{v} & \boldsymbol{0} \\ \boldsymbol{v} & \boldsymbol{v} & \boldsymbol{1-v} & \boldsymbol{0} \\ \boldsymbol{0} & \boldsymbol{0} & \boldsymbol{0} & \dfrac{\boldsymbol{1-2v}}{\boldsymbol{2}} \end{bmatrix} \qquad (\boldsymbol{Equation\ 35})$$

The seismic force will be formulated as the product of the stiffness matrix and the applied seismic excitation according to the earthquake records.

$$\{\boldsymbol{Fs}\} = [\boldsymbol{M}] \times \{\boldsymbol{\alpha g}\} \qquad (\boldsymbol{Equation\ 36})$$

The main objective in dynamic analysis is to determine the pore water pressure induced by the seismic force in order to identify potential liquefaction zones.

CHAPTER 4

RESULTS AND DISCUSSIONS

4.1 Depression Curve Results

The conclusions of the depression curve have also been compared with the water levels provided in the geological profile. The result of the depression curve profile analysis from the program used (GeoStudio 12) is presented below:

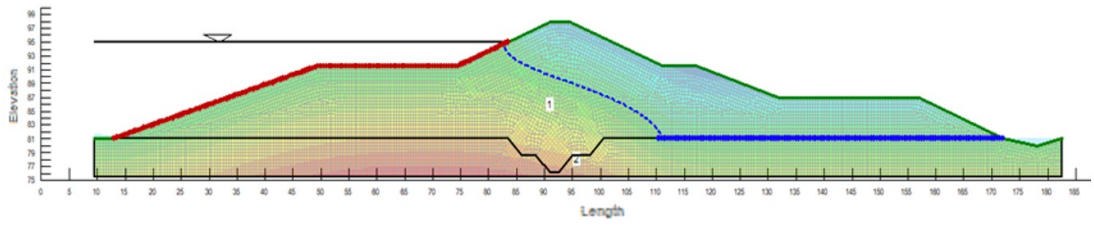

Figure 10. Depression curve model

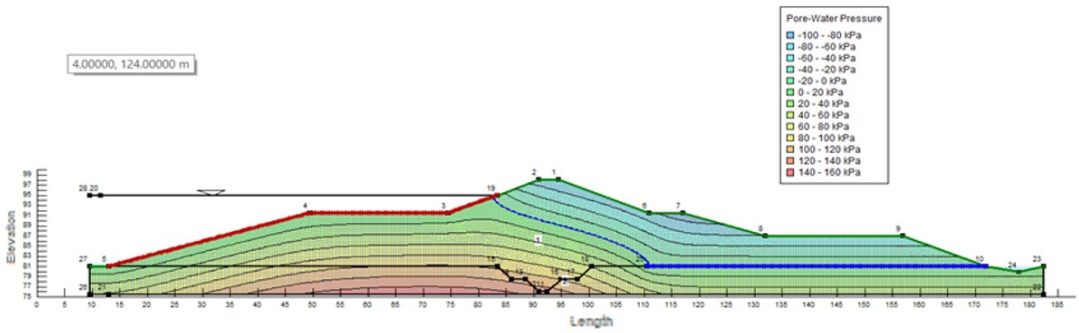

Figure 11. Depression curve model & pore pressure

4.2 Reservoir Emptying and Pore Pressure Results

The drainage time of the reservoir according to the current situation is t = 4.22 days.

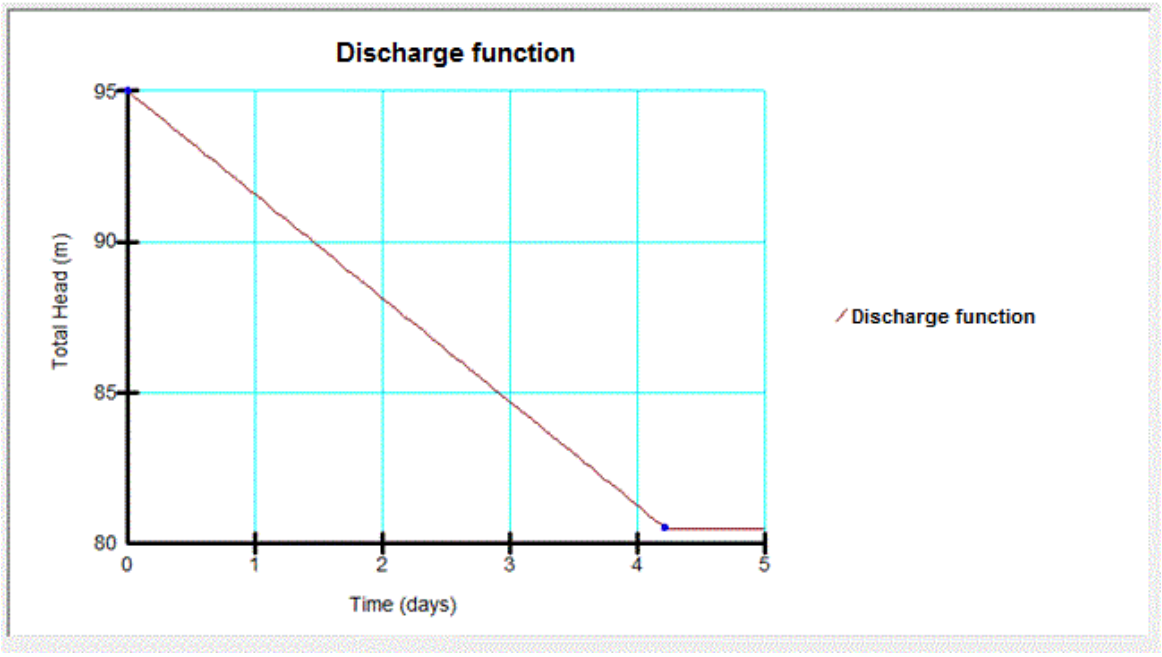

Figure 12. Discharge Function

For the time t = 0.0 hours of drainage, we have the following results for the water pore pressure:

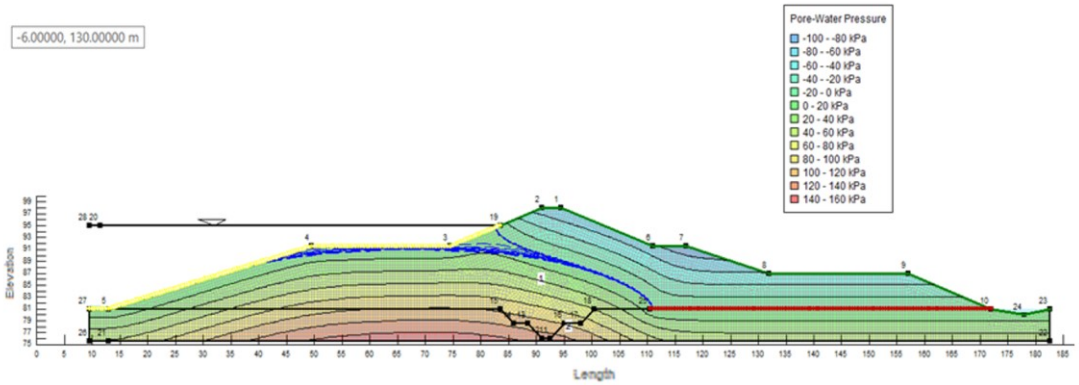

Figure 13. Pore pressure in t = 0 of dam emptying

For the time t = 4.22 days of drainage, we have the following results for the water pore pressure:

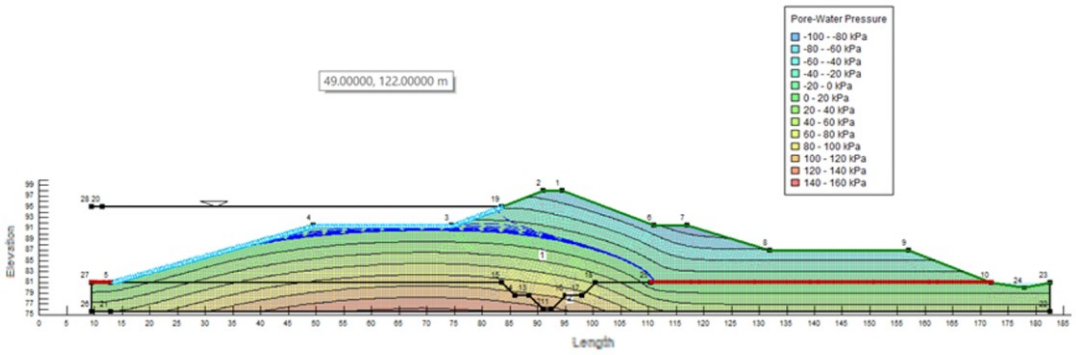

Figure 14. Pore pressure in t = 4.22 days of dam emptying

Let's assume that the drainage time from the maximum level to the minimum level of the dam will increase from t = 4.22 days to t = 20 days according to the following graph:

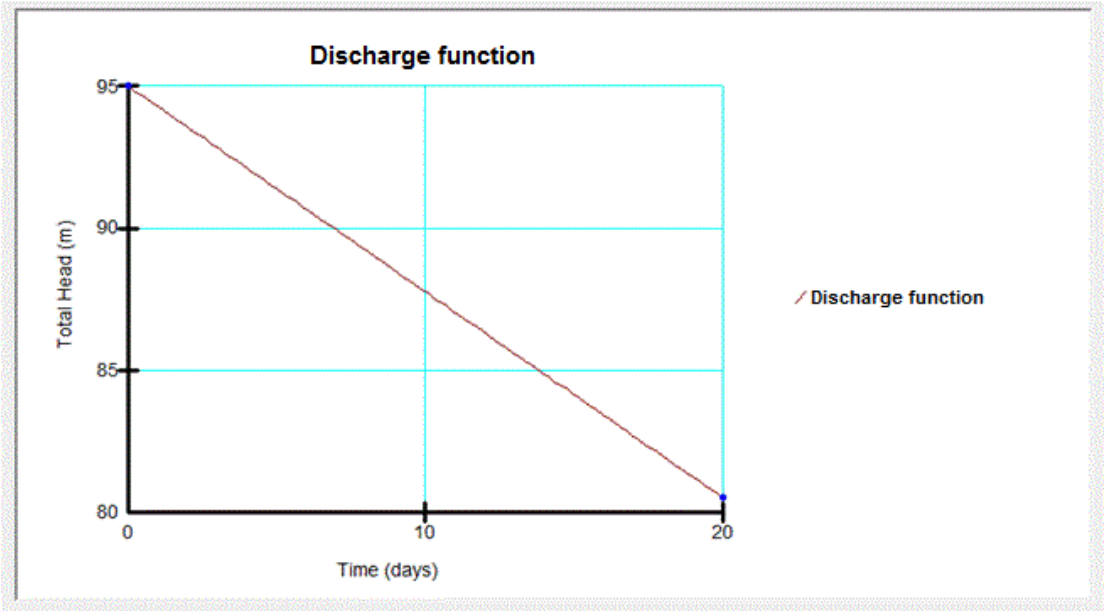

Figure 15. Drainage graph for t = 20 days

For the time t = 4.22 days from the beginning of drainage, we have the results of water pore pressure as follows:

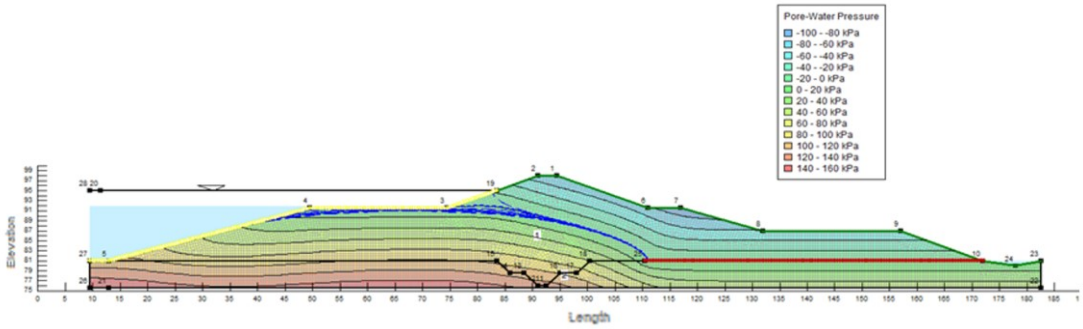

Figure 16. Pore pressure in t = 4.22 days from the beginning of dam emptying

For the time t = 8 days from the beginning of drainage, we have the results of water pore pressure as follows:

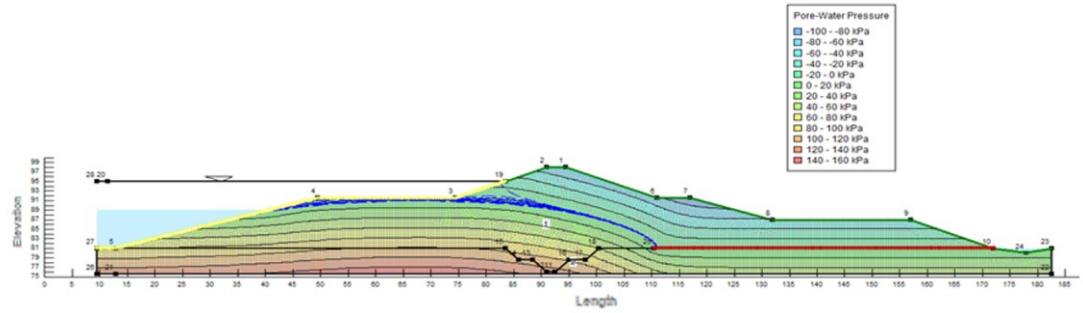

Figure 17. Pore pressure in t = 8 days from the beginning of dam emptying

For the time t=15 days from the beginning of drainage, we have the results of water pore pressure as follows:

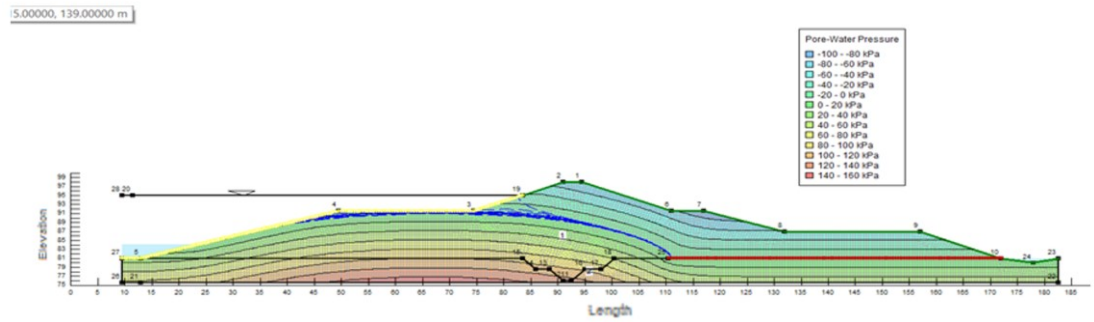

Figure 18. Pore pressure in t = 15 days from the beginning of dam emptying

For the time t = 20 days from the beginning of drainage, we have the results of water pore pressure as follows:

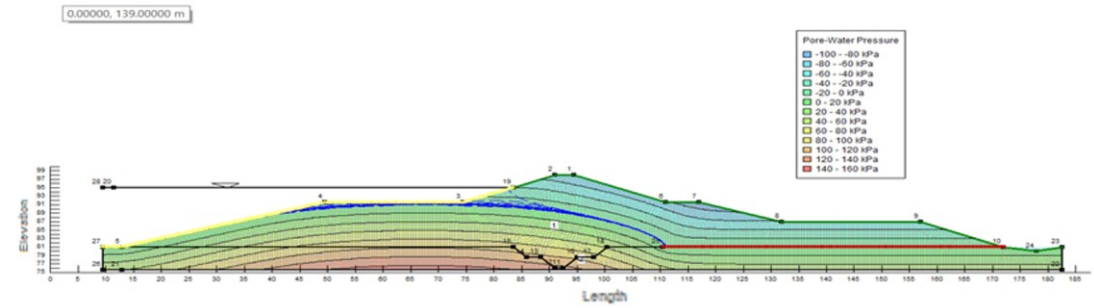

Figure 19. Pore pressure in t = 20 days from the beginning of dam emptying

4.3 Factor of safety

The stability assessment of slopes in the upper and lower sections has been conducted for both scenarios as follows:

- Scenario 1: The pore pressure remains constant.

- Scenario 2: The pore pressure changes over time (immediate drawdown of water in the reservoir).

In scenario 1, the slope stability in the upper section is ensured with a critical factor of safety (FoS) value of 2.364, while in the lower section, the critical FoS value is 2.226.

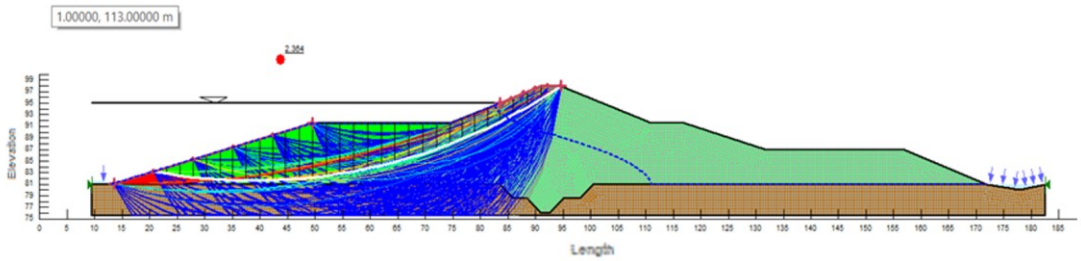

Figure 20. Upper slope factor of safety due to constant pore pressure

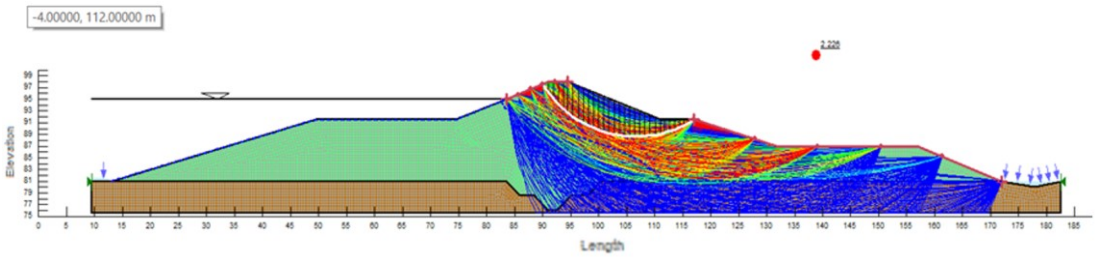

Figure 21. Lower slope factor of safety due to constant pore pressure

In scenario 2, the variation of pore pressure has been analysed for two cases in the upper slope:

A) The first case considers the change in pore pressure when the water level in the reservoir undergoes a maximum-minimum drawdown for 13.1 hours or 0.54 days, according to calculations by the water management system.

B) The second case examines the pore pressure variation in the upper slope when the water level in the reservoir experiences a maximum-minimum drawdown for 14-15 days.

In the first case (A), with a duration of 4.22 days, the factor of safety is determined to be FoS = 2.385.

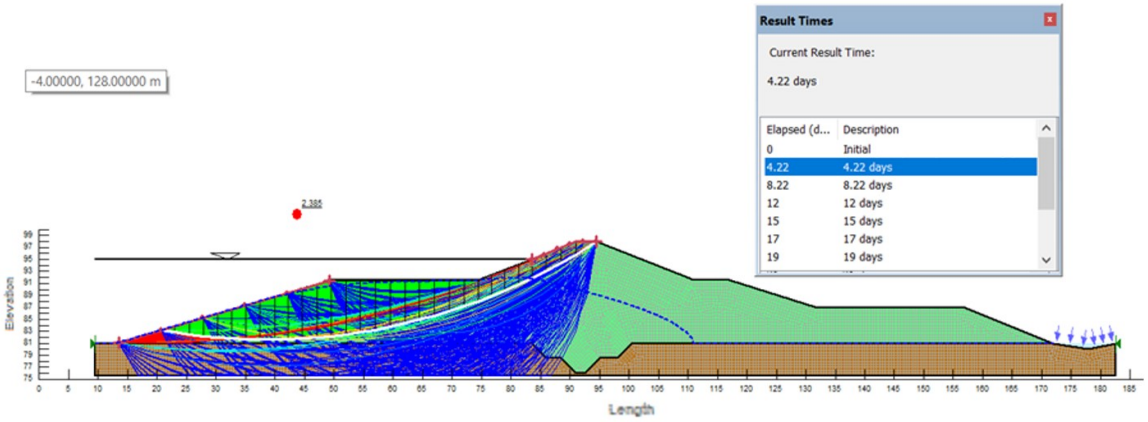

Figure 22. Upper slope factor of safety, scenario A, due to non-constant pore pressure

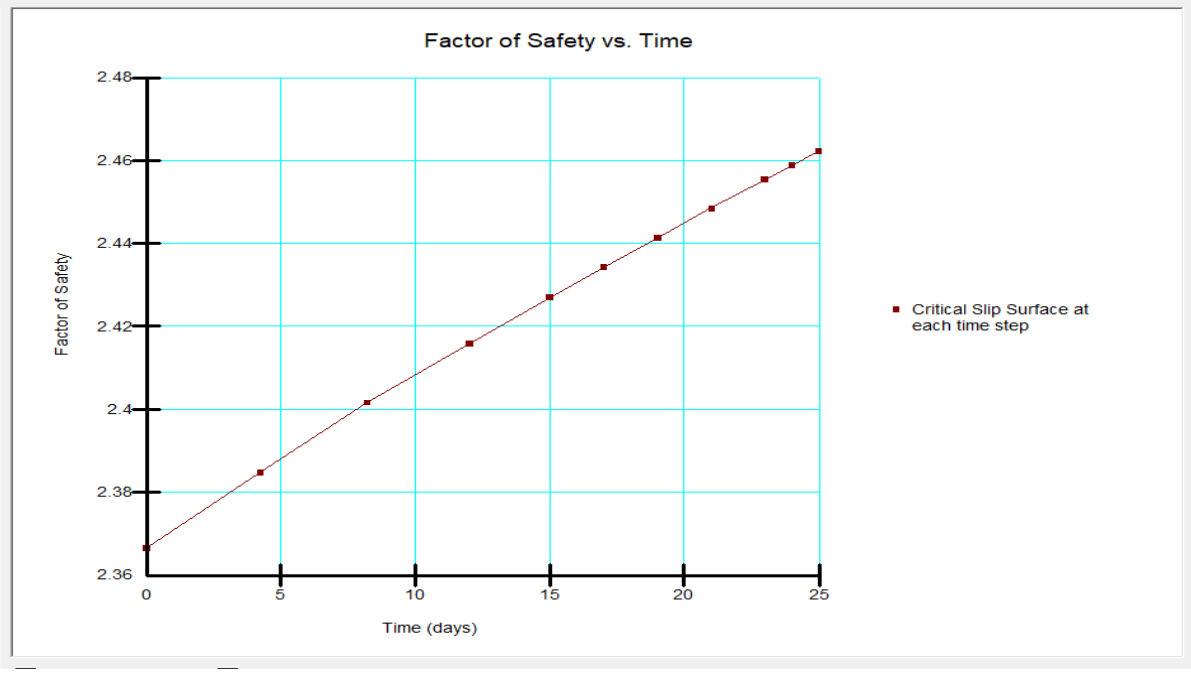

Figure 23. Change of the factor of safety in upper slope, scenario A, due to non-constant pore pressure

In the second case (B), with a duration of 20 days, the factor of safety is determined to be FoS = 3.243.

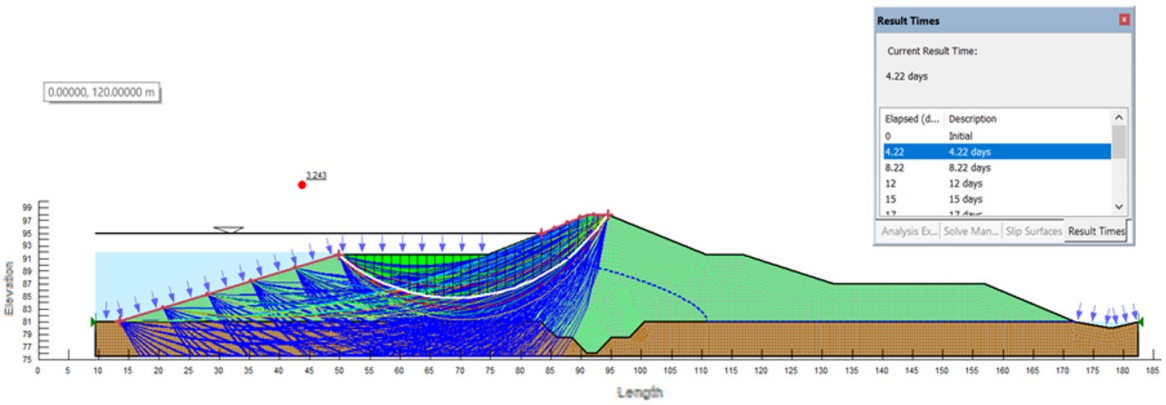

Figure 24. Upper slope factor of safety, scenario B, due to non-constant pore pressure

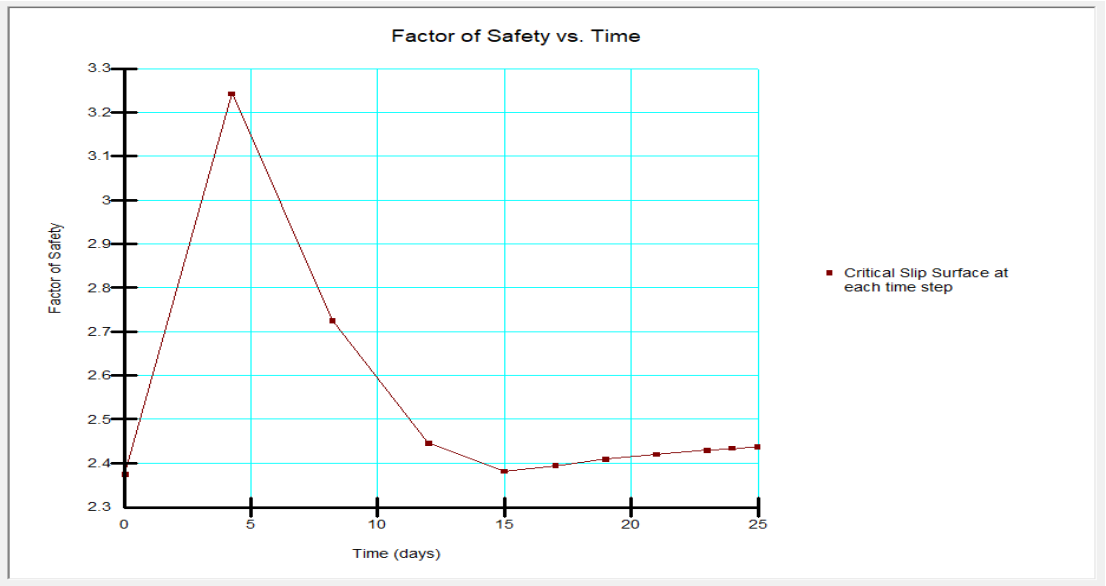

Figure 25. Change of the factor of safety in upper slope, scenario B, due to non-constant pore pressure

As observed, the increase in the reservoir drainage time influences the improvement of the factor of safety in the upper slope. Comparing graphs Figure 23 and Figure 25, the factor of safety increases by approximately 26.4%, and even more as time progresses, since the negative pore water pressure will be created within the soil structure, leading to an increase in the resisting force of the soil.

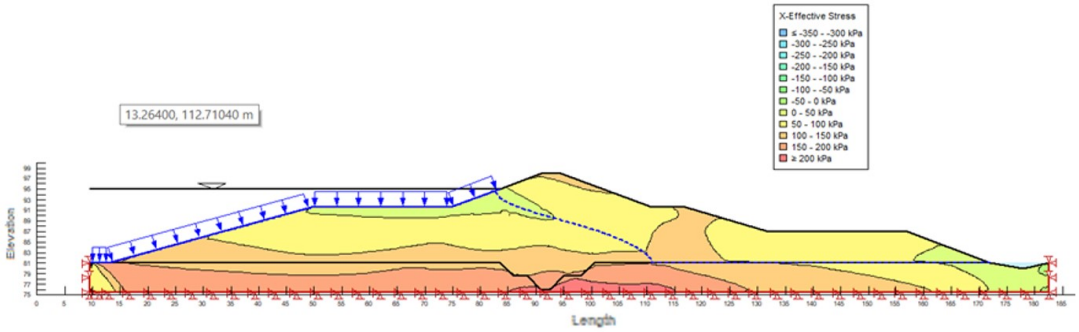

Figure 26. Static scheme in stress/strain analysis

The fundamental equation of effective stresses has been calculated in the computer program using GeoStudio 12, and the results are as follows:

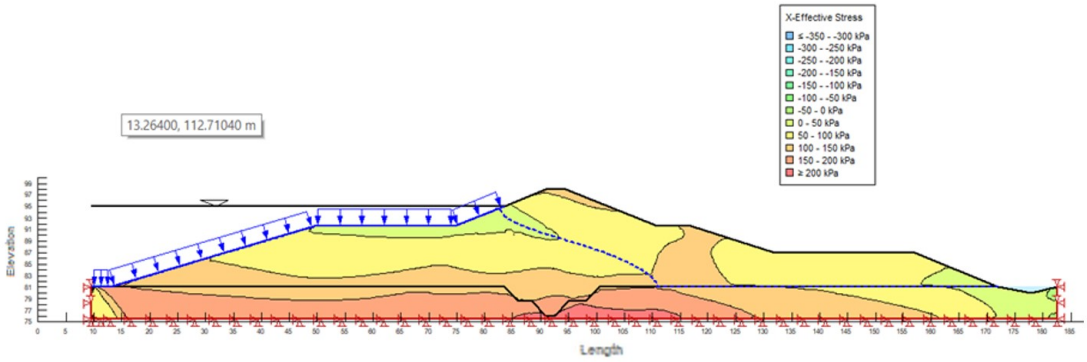

Figure 27. Horizontal effective stresses

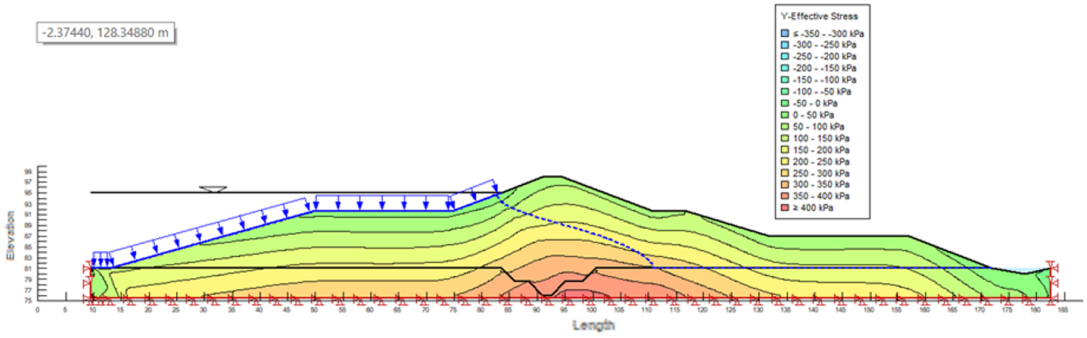

Figure 28. Vertical effective stresses

Below are the results of the factor of safety for the lower slope before seismic action.

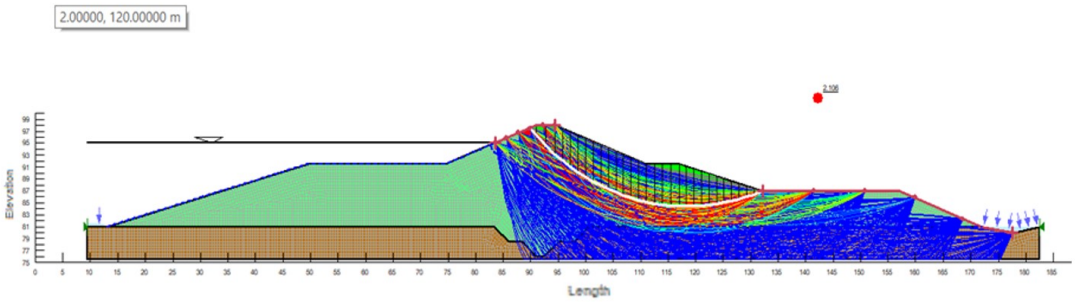

Figure 29. Lower slope factor of safety before seismic load

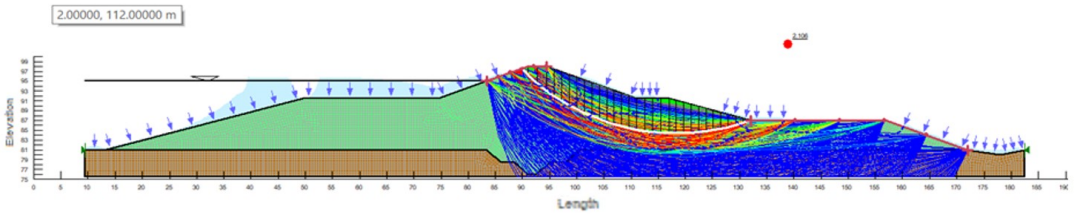

Figure 30. Lower slope factor of safety after seismic load

4.4 Seismic Activity Analysis Results

Dynamic analysis is another important part in order to conduct a stability analyses. The dynamic energy released from earthquakes transfer their energy to pores of the soil. This results on the increase of the pressure, which may lead to liquification failure of the soil. The seismic analyses results on 3 graphs, which interpretates the increase of pore pressure, high potential liquification zones and the relative displacement, as shown below.

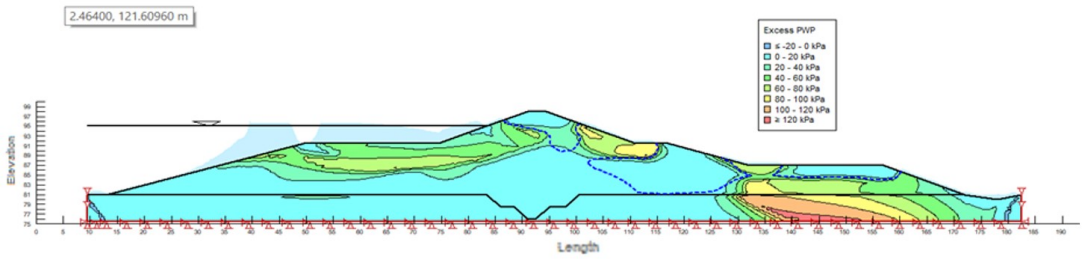

Figure 31. Graph of pore pressure after seismic load

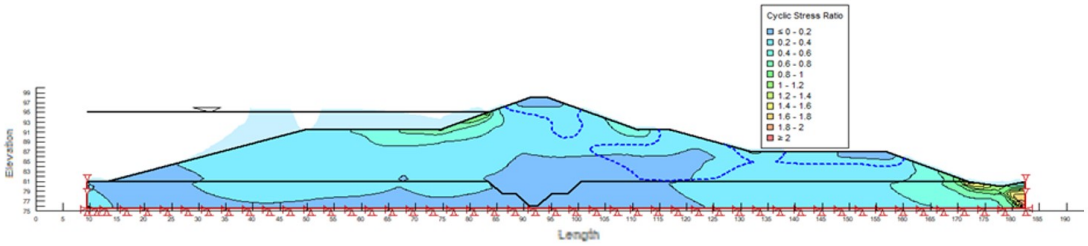

Figure 32. High potential liquification zones

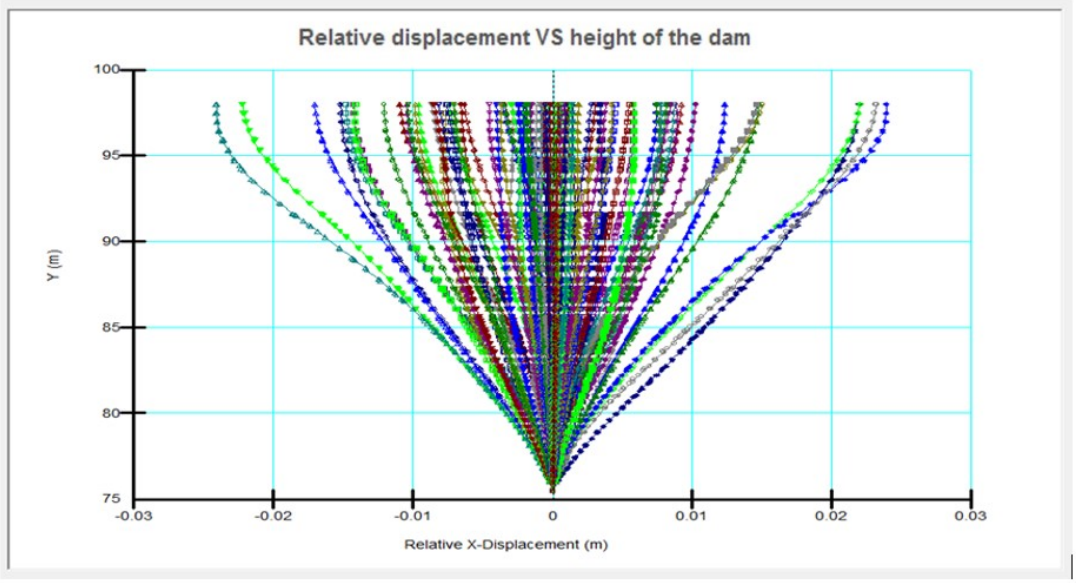

Figure 33. Graph of horizontal displacement due to height

CHAPTER 5

CONCLUSIONS

5.1 Conclusions

Based on the stability analysis, the following conclusions have been reached:

1. The stability of the slopes under hydrostatic forces of the Cerkeze dam is identified in a state of stable equilibrium.

2. Static analysis of effective stresses identifies values that, compared to those obtained in the geological thesis, fall within acceptable ranges.

3. Dynamic analysis has identified a decrease in the factor of safety for the lower and upper slopes of the Cerkeze dam compared to static values. However, they remain in a state of equilibrium within the limits of stability, considering the additional seismic forces with a recurrence period of 975 years. Nevertheless, it is recommended to improve and reinforce the lower slope of the dam with Rip-Rap concrete layers and enhance the upper slope with a reinforced concrete layer and anchoring with tensioned anchors on the concrete surface.

4. Horizontal displacements along the axis of the Cerkeze dam are within allowable limits.

5. The construction of a reinforced concrete screen in the upper basin is necessary for slope stability. The main reason is the permeability parameter, especially in dams with clay materials, which have a very low permeability. In a very short period of immediate drawdown of the water level, the pore water pressure will remain positive. This means that the resistance of the material in the upper slope will decrease, resulting in reduced stability.

6. Stabilizing the lower slope by predicting reinforced concrete layers connected together will improve the factor of safety parameters and bring the slope to

a stable equilibrium, mitigating both surface and internal erosion caused by activities within the dam.

REFERENCES

[1] B. o. Reclamation, "RCEM - Reclamation Consequence Estimating Methodology," June 2015. [Online]. Available: https://www.usbr.gov/ssle/damsafety/documents/RCEM-CaseHistories2015.pdf.

[2] "KKDM ALBCOLD," 4 6 2021. [Online]. Available: albcold.gov.al.

[3] U. Obinna, "Earth Dams: Types, construction and modes of failure," 2021.

[4] A. University, "BrainKart," [Online]. Available: www.brainkart.com.

[5] D. v. Zyl, "Embankment Dams, Seepage, Filter Design and Critical Gradient," *Mine Waste Management,* 2013.

[6] T. Stephens, Manual on small earth dams, 1951.

[7] A. H. Bhutto, "STABILITY OF EMBANKMENT DAMS UNDER STATIC," *STABILITY OF EMBANKMENT DAMS UNDER STATIC,* 2020.

[8] B. o. Reclamation, "Embankment Dams," in *Embankment Dams*, U.S . Department of the Interior, 2012, pp. 32-47.

[9] E. C. f. Standardization, "Eurocode 7," in *Eurocode 7*, Brussels, rue de Stassart, 36, 2004, pp. 19-36.

[10] E. C. f. Standardization, "Eurocode 8," in *Eurocode 8*, Brussels, rue de Stassart, 2004, pp. 33-46.

[11] S. Sahlin, Structural Masonry, Englewood Cliffs, New Jersey: Prentice-Hall Inc., 1971.

[12] ASTM, "ASTM C 270-03, Standard Specification for Mortar for Unit Masonry," ASTM International, West Conshohocken, PA, 2003.

[13] S. V. Deodhar, "Strength of Brick Masonry Prisms in Compression," *Journal of the Institution of Engineers (India),* vol. 81, no. 3, pp. 133-137, 2000.

[14] CEN, "EN 1996-1-1: Design of masonry structures - Part 1-1: General rules for reinforced and unreinforced masonry structures."," European Committee for Standardization, Brussels, Belgium, 2005.

[15] P. B. Lourenço, Computational strategies for masonry structures, Delft, Netherlands: Delft University of Technology, 1996.

[16] D. S. P. M. G. B. R. Fell, Geotechnical Engineering of Dams, Netherlands: A.A. Balkema Publishers Leiden, 2005.

[17] S. P. R.C. Hirschfeld, Embankment Engineering - Casagrande, New York: Wiley Interscience, 1973.

[18] B. o. Reclamation, "Dam Safety Public Protection Guidelines," August 2011. [Online]. Available: http://www.usbr.gov/ssle/damsafety/documents/PPG201108.pdf.

[19] M. F. R. a. S. M. Foster, "The statistics of embankment dam failures and accidents," *Canadian Geotechnical Journal,* vol. 37, 2000.

[20] E. a. H. S. Panulinova, "Methods for analyzing the stability of an earthen dam slope," *Advanced Materials Research,* vol. 969, 2014.

[21] E. Spencer, "A method of analysis of the stability of embankments assuming parallel inter-slice forces," *Geotechnique,* vol. 17, pp. 11-26, 1967.

[22] A. A. S. P. S. R. R. a. M. D. Burman, "A comparative study of slope stability analysis using traditional limit equilibrium method and finite element method," *Asian journal of civil engineering (building and housing),* vol. 16, no. 4, pp. 467-492, 2015.

[23] D. a. P. L. Griffiths, "Slope stability analysis by finite elements," vol. 49, no. 3, pp. 387-403, 1999.

[24] M. M. Berilgen, "Investigation of stability of slopes under drawdown conditions," vol. 49, no. 3, pp. 81-91, 2007.

[25] M. L. H. a. F. T. Fredlund, Combined seepage and slope stability analysis of rapid drawdown scenarios for levee design, Geo-Frontiers, 2011.

[26] D. Vandenberge, "Total stress rapid drawdown analysis of the Pilarcitos Dam failure using finite element method," vol. 8, no. 2, pp. 115-123, 2014.